Synergistic anti-tumor activity of miriplatin and radiation through PUMA-mediated apoptosis in hepatocellular carcinoma

Hironori Tanaka[1], Koichi Okamoto[1], Yasushi Sato[1], Takahiro Tanaka[1], Tetsu Tomonari[1], Fumika Nakamura[1], Yasuteru Fujino[1], Yasuhiro Mitsui[1], Hiroshi Miyamoto[1], Naoki Muguruma[1], Akinori Morita[2], Hitoshi Ikushima[3], Tetsuji Takayama[1]

1) Department of Gastroenterology and Oncology, Tokushima University Graduate School of Biomedical Scinces, 3-18-15 Kuramoto-cho, Tokushima 770-8503, Japan

2) Department of Biomedical Science and Technology, Tokushima University Graduate School of Biomedical Sciences, 3-18-15 Kuramoto-cho, Tokushima 770-8503, Japan

3) Department of Therapeutic Radiology, Tokushima University Graduate School of Biomedical Sciences, 3-18-15 Kuramoto-cho, Tokushima 770-8503, Japan

Short title: Chemoradiotherapy with miriplatin

Address correspondence to Tetsuji Takayama, M.D., Ph.D., 3-18-15, Kuramoto-cho, Tokushima, 770-8503, Japan. Tel: +81-88-633-7124. Fax: +81-88-633-9235.

E-mail: takayama@tokushima-u.ac.jp

5996 words

Abstract

Background: The prognosis for patients with unresectable advanced hepatocellular carcinoma (HCC) is poor. Miriplatin is a hydrophobic platinum compound that has a long retention time in lesions after transarterial chemoembolization (TACE). We investigated anti-tumor activity of miriplatin combined with irradiation on HCC cells, and its underlying mechanism of apoptosis. We also analyzed the effectiveness of miriplatin-TACE and radiotherapy for locally advanced HCC.

Methods: Human HCC cell lines HepG2 and HuH-7 were treated with DPC (active form of miriplatin) and radiation, and synergy was evaluated using a combination index (CI). Apoptosis-related proteins and cell cycles were analyzed by western blotting and flowcytometry. We retrospectively analyzed treatment outcomes in 10 unresectable HCC patients with vascular/bile duct invasion treated with miriplatin-TACE and radiotherapy.

Results: DPC or X-ray irradiation decreased cell viability dose-dependently. DPC plus irradiation decreased cell viability synergistically in both cell lines (CI<1 respectively). Cleaved PARP expression was induced much more strongly by DPC plus irradiation than by each treatment alone. Expression of p53 up-regulated modulator of apoptosis (PUMA) was significantly induced by the combination, and knockdown of PUMA with siRNA significantly decreased apoptosis in both cell lines. DPC plus irradiation caused sub-G1, G2/M, and S phase cell arrest in those cells. The combination of miriplatin-TACE and radiotherapy showed a high response rate for patients with locally advanced HCC despite small number of patients.

Conclusions: Miriplatin plus irradiation had synergistic anti-tumor activity on HCC cells through PUMA-mediated apoptosis and cell cycle arrest. This combination may possibly be effective in treating locally advanced HCC.

Key words: hepatocellular carcinoma, miriplatin, radiation, synergistic effect, apoptosis

Introduction

Hepatocellular carcinoma (HCC) is the fourth-leading cause of cancer-related death worldwide [1]. Most patients with HCC are diagnosed at an advanced stage, when curative therapies, such as surgical resection and percutaneous ablation, are of limited utility. A majority of HCCs exhibit intrinsic resistance to many cytotoxic anti-cancer agents and, therefore, interventional treatments such as transarterial chemotherapy have been applied for advanced HCC [2, 3]. Recently, the therapeutic efficacy of systemic treatment with sorafenib, a tyrosine kinase inhibitor, on unresectable HCC was reported; sorafenib significantly improved overall survival (OS) in patients with unresectable advanced HCC in randomized controlled phase III trials [4]. More recently, other tyrosine kinase inhibitors such as regorafenib and lenvatinib were reported to be effective for the treatment of advanced HCC [5, 6]. However, a serious limitation of these multi-kinase inhibitors is that they show poor efficacy for treating HCCs that invade the major portal vein, hepatic vein, or bile duct. Therefore, the prognosis for these locally advanced HCC is extremely poor [7, 8]. For example, Cheng and associates reported that the median survival time for cases of HCC with major vascular invasion was only 5.6 months despite treatment with sorafenib [9].

With recent advances in three-dimensional radiation techniques, radiotherapy has become a treatment option for unresectable HCC. In particular, radiotherapy has been reported to be effective for treatment of portal vein and/or inferior vena cava tumor thrombosis in HCC [10, 11]. Moreover, transarterial chemoembolization (TACE) combined with radiotherapy was reported to be effective in treating HCC with portal vein tumor thrombus [12]. Notably, Yoon and associates reported that TACE with cisplatin (CDDP) combined with radiotherapy was very effective for the treatment of unresectable HCC invading the portal vein; the response rate (RR) and median overall

survival (OS) were 39.6% and 10.6 months, respectively [13]. In a randomized clinical trial, the same group showed that TACE with CDDP combined with radiotherapy was superior to sorafenib for the treatment of HCC with macroscopic vascular invasion [14]. However, these outcomes with respect to RR and OS of treatment with TACE with CDDP and radiotherapy remain unsatisfactory. In addition, CDDP has various adverse effects such as renal toxicity, vascular damage, and GI toxicity, and it shows poor tumor retention when administered as TACE [15, 16].

Miriplatin (cis-[1R,2R]-1,2-cyclohexanediamine-N,N']bis[myristate])-platinum(II) monohydrate; Sumitomo Dainippon Pharma Co, Ltd. Osaka, Japan) is a novel lipophilic anti-cancer drug that can be suspended in lipiodol, a lipid lymphographic agent for TACE [16], and it is less toxic and has a much longer retention time in tumor tissues compared with CDDP. A phase II study of TACE with miriplatin and iodized oil showed promising efficacy for unresectable HCC with a mild toxicity profile [17]. Subsequent studies of TACE with miriplatin also revealed better efficacy and much lower toxicity for the treatment of unresectable HCC compared with other anti-cancer agents, despite a few contradictory reports [18, 19]. However, combination therapy with miriplatin and radiotherapy for HCC has not been studied to date. Therefore, in this study, we first investigated the anti-cancer activity and synergistic effect of miriplatin plus X-ray combination therapy using HCC cell lines. Since we ultimately observed synergistic anti-tumor activity with this combination, we next examined the underlying mechanism of synergistic activity, including apoptosis, using HCC cell lines. We also evaluated the anti-tumor activity of TACE with miriplatin combined with radiotherapy in HCC patients with vascular and/or bile duct invasion.

MATERIALS AND METHODS

Cell culture

The human HCC cell lines HepG2 and HuH-7 were purchased from American Tissue Culture Collection. Cells were maintained in DMEM supplemented with 10% fetal bovine serum (FBS).

Drugs and reagents

Miriplatin and dichloro [(1R, 2R)-1,2-cyclohexanediamine-N, N'] platinum (DPC), an active form of miriplatin, were provided by Sumitomo Dainippon Pharma Co, Ltd. DPC was dissolved in N,N-dimethylformamide (DMF) and CDDP (Sigma-Aldrich, St Louis, MO) was dissolved in saline.

Radiation exposure

Cells were irradiated in the medium at room temperature with an X-ray generator (MBR-1520R-3, Hitachi, Japan) operating at 150 kV–20 mA with a filter of 0.1 mm Cu and 0.5 mm Al at a dose rate of 1.0 Gy/min.

Cell viability assay

Cell viability was examined by WST-8 assay, according to manufacturer's instructions.

Calculation of Combination index (CI)

DPC or CDDP was added to the cells at a concentration of 0 – 10 μM, and the cells were irradiated with X-rays at 0 – 10 Gy. They were subsequently incubated at 37ºC for 120 h and cell viability was determined by WST-8 assay to generate a new cell viability curve. Based on these data, a combination index (CI) was calculated

according to the method of Chou and Talalay using CompuSyn software (ComboSyn, Paramus, NJ) [20, 21]. The CI value was plotted against the fraction of affected cells (Fa), which represents the percentage of growth inhibition (CI-Fa plot). Three independent experiments consisting of quintuplicate assays for each condition were performed to generate CI-Fa plots. A CI value < 1.0 indicates synergism of the combination.

Western blot analysis

Expression of apoptosis-related proteins was analyzed by western blot analysis, as described previously [22]. The primary antibodies used are listed in Supplementary Table 1.

Cell cycle analysis

Cell cycle was analyzed using a Cell Cycle Phase Determination Kit (Cayman chemical, Ann Arbor, MI) according to manufacturer's instruction. Briefly, cells were seeded in 10-cm dishes and the culture medium was changed to serum-free medium for 24 h to facilitate cell cycle synchronization. DPC was added to the wells with or without irradiation. After incubation for 24 h, the DNA content of propidium iodide (PI)-stained cell nuclei was determined using a BD FACSVerse flow cytometer (BD Biosciences, San Jose, CA). For analysis of DNA synthetic activity, BrdU assay was performed using an FITC BrdU Flow Kit (BD Biosciences), according to manufacturer's instructions.

Retrospective study of TACE with miriplatin combined with radiotherapy for unresectable HCC with portal/hepatic and/or bile duct invasion

We retrospectively analyzed the anti-tumor effect of TACE with miriplatin or CDDP combined with radiotherapy for patients with HCC between February 2012 and April 2019 at Tokushima University Hospital. The criteria for enrollment were as follows; (i) unresectable HCC that macroscopically invaded the major branch of the portal vein (Vp1 - 3), hepatic vein (Vv1 - 3) or bile ducts (B1 - 4) in contrast-enhanced CT; and (ii) Child–Pugh classification A or B. Patients with extrahepatic metastasis or with invasion to the main trunk of the portal vein were excluded. A total of 10 patients in the miriplatin group and 15 patients in the CDDP group who satisfied the eligibility criteria were evaluated. This study was approved by the institutional review board of our university.

We evaluated primarily the main tumor with vascular/bile duct invasion inside the radiation field by serial CT scans performed 3 months after the completion of TACE and radiotherapy, according to criteria described previously [23], as follows: complete response (CR), complete disappearance of tumor; partial response (PR), >30% reduction of tumor in the largest diameter without complete disappearance of tumor; progressive disease (PD), >20% extension of tumor in the largest diameter; stable disease (SD), neither sufficient regression to qualify for PR nor sufficient growth to qualify for PD. We also evaluated secondarily intrahepatic nodules outside the radiation field according to modified RECIST criteria [24]. OS was measured from the date of initial treatment to the date of death or last follow-up and assessed by the Kaplan–Meier method.

Detailed information on the method for clonogenic cell survival assay, apoptosis assay, siRNA transfection, and TACE with radiotherapy is provided in Supplementary Methods and Results.

Results

Anti-tumor activity of DPC, CDDP and X-ray irradiation on hepatocellular carcinoma cell lines

We first analyzed the anti-tumor effect of DPC, an active form of miriplatin, and CDDP on HepG2 and HuH-7 cells by cell viability assay. The viability of HepG2 cells treated with DPC or CDDP decreased in a dose-dependent manner. The IC50 values for DPC and CDDP were 3.66 ± 1.45 and 6.30 ± 1.66 μM respectively; i.e., the IC50 of DPC was significantly lower than that of CDDP (p<0.03 by Student's t test; Fig.1A). Similarly, the IC50 of DPC in HuH-7 cells (0.90 ± 0.34 μM) was significantly lower than that of CDDP (5.84 ± 1.07μM, p<0.01). Thus, DPC exhibited greater anti-tumor activity than CDDP against both HCC cell lines.

When HepG2 or HuH-7 cells were irradiated with X-rays at 0 – 10 Gy, cell viability decreased in a dose-dependent manner, with ED50s of 5.6 Gy and 5.2 Gy, respectively (Supplementary Fig.1A).

Synergistic effect of DPC and X-ray irradiation on HCC cells

To evaluate the synergistic effect of anti-tumor drug treatment and X-ray irradiation, we examined the viability of HepG2 and HuH-7 cells using the combination index method after treatment with various concentrations of DPC or CDDP in combination with 0 – 10 Gy X-ray irradiation. HepG2 and HuH-7 cell viability decreased in a dose-dependent manner following treatment with DPC in each X-ray dose group from 0 – 10 Gy (Fig.1B,C). Moreover, the viability curve for each X-ray exposure group gradually decreased with increasing X-ray doses. The Chou and Talalay (CI – Fa) plot revealed that all the CI values were less than 1.0 in the range of Fa ≥0.2 in HepG2 and HuH-7 cells, clearly showing a downward trend of CI values with increasing Fa.

Since it is well known that synergism (CI value) at higher Fa levels is more relevant to the anti-cancer therapeutic effect than that at lower Fa levels [20, 25], DPC and X-ray irradiation were judged to have synergistic effects in both cell lines. In contrast, for CDDP plus X-ray irradiation only one CI value was less than 1.0 (around 0.6 of Fa) but the other 3 CI values (including the one at the highest Fa level) were greater than 1.0, failing to show a downward trend of CI values with increasing Fa in both cell lines (Fig.1D,E). Thus, CDDP plus X-ray irradiaition was judged to have little synergy or a very weak synergistic effect.

To evaluate the long-term combination effect of DPC and X-ray irradiation, we performed colony forming assays in HepG2 and HuH-7 cells. Representative images of colonies in each HepG2 treatment group are shown in Fig.2A. The number of colonies of HCC cells formed was lowest in cells treated with DPC plus X-ray irradiation as compared with all other treatment groups, although the number of colonies formed in cells treated with DPC or X-ray irradiation alone was also lower compared with control cells. Mean clonogenic survival (percentage of control cells) in the DPC plus X-ray irradiation group (38.3 ± 2.1) was significantly lower than that in the DPC alone (51.7 ± 3.0) and X-ray irradiation alone groups (86.8 ± 3.7) (p<0.05 respectively, by Turkey's test; Fig.2B). Mean clonogenic survival in the latter 2 groups was significantly lower compared with control cells (p<0.05 respectively). Similar results were obtained in the colony forming assay with HuH-7 cells (Fig.2C,D; p<0.05 respectively).

Apoptosis induction with DPC plus X-ray irradiation

To investigate the mechanism of the synergistic anti-tumor effect of the combination treatment on HCC cells, apoptosis was examined by western blotting and

flow cytometry in HCC cells treated with DPC and/or X-ray irradiation, in comparison with CDDP and/or X-ray irradiation. When HepG2 and HuH-7 cells were treated with various concentrations of DPC or CDDP, the expression of cleaved PARP and caspase-3 was induced in a dose-dependent manner at 0 – 20 μM (including low concentrations of 0 – 5 μM) in both cell lines (Supplementary Fig.2A,B). Moreover, cleavage of PARP and caspase-3 was also induced in both cell lines in a dose-dependent manner after treatment with X-ray irradiation alone (Supplementary Fig.1B). When HepG2 and HuH-7 cells were treated with DPC plus X-ray irradiation, the induction of cleaved PARP and caspase-3 expression was much stronger than with each treatment, and with CDDP plus X-ray irradiation, suggesting that the synergistic anti-tumor effect of DPC plus X-ray irradiation is caused by apoptosis in both cell lines (Fig.3A).

In the flow cytometry analysis, the percentage of annexin V (+) in HepG2 cells treated with DPC plus X-ray irradiation (53.5 ± 1.7%) was significantly higher compared with control cells treated with vehicle alone (11.4 ± 0.4%; $p<0.01$ by Turkey's test) or CDDP plus X-ray irradiation (33.1 ± 2.4%; $p<0.01$; Fig.3B). Similarly, the percentage of annexin V (+) in HuH-7 cells treated with DPC plus X-ray irradiation (50.8 ± 1.0%) was significantly higher than that with vehicle treatment alone (13.2 ± 1.6%, $p<0.01$) or CDDP plus X-ray irradiation (41.5 ± 1.5%; $p<0.01$; Fig.3C).

Mechanism of synergistic effect of DPC and X-ray irradiation

To further investigate the mechanism of apoptosis induction by DPC and X-ray irradiation, we examined the expression of major apoptosis-related proteins (Bim, Bik, p53 up-regulated modulator of apoptosis [PUMA], Noxa, Bcl-2, Mcl-1, and Bcl-xl) in HepG2 and HuH-7 cells by western blot analysis. When HepG2 cells were treated with

DPC alone, PUMA expression was significantly increased in a dose-dependent manner at 0 – 20 μM (including low concentrations of 0 – 5 μM), whereas expression of Bim, Bik, Noxa, Bcl-2, Mcl-1, and Bcl-xl did not change significantly (Supplementary Fig.2A). Conversely, PUMA expression was not changed by treatment with CDDP, irrespective of the concentration, suggesting that the mechanism of apoptosis induction by CDDP differs from that of DPC. Moreover, when HepG2 cells were treated with DPC plus X-ray irradiation, PUMA expression was much stronger than that of each treatment individually, whereas the expression of other apoptosis-related proteins did not change significantly (Fig.4A and Supplementary Fig.3). Quantitative imaging analysis showed that the PUMA expression level (PUMA/β-actin ratio) of HepG2 cells treated with DPC plus X-ray irradiation was significantly higher than that with treatment with DPC, X-ray irradiation alone, or CDDP plus X-ray irradiation, as well as control cells (Fig.4B). Similarly, PUMA expression was significantly increased in a dose-dependent manner in HuH-7 cells after treatment with DPC, whereas it did not change after treatment with CDDP (Supplementary Fig.2B). Moreover, PUMA expression of HuH-7 cells treated with DPC plus X-ray irradiation was significantly higher than with treatment with DPC, X-ray irradiation alone, or CDDP plus X-ray irradiation, as well as control cells (Fig.4C,D). These results indicate that PUMA plays a critical role in the induction of apoptosis by DPC and X-ray irradiation in combination.

To investigate the mechanism of PUMA induction, we examined the expression of JNK, c-Jun, and CHOP expression in HepG2 and HuH-7 cells by western blotting. Expression of p-JNK and p-c-Jun in HepG2 cells after treatment with DPC plus X-ray irradiation was significantly higher compared with control cells and cells after treatment with CDDP plus X-ray irradiation (Fig.4E). However, expression of ER stress-related protein (CHOP) did not change after treatment with DPC plus X-ray irradiation or

CDDP plus X-ray irradiation. Similar results were obtained in HuH-7 cells after treatment with DPC plus X-ray irradiation (Fig.4F). These results suggest that the combination of DPC plus X-ray irradiation induced PUMA expression dependent on the JNK signaling pathway.

To confirm the role of PUMA in the synergistic effect of DPC and X-ray irradiation, we knocked down the PUMA gene in HepG2 and HuH-7 cells using siRNA and examined changes of apoptosis. The relative mRNA levels of PUMA in the knocked-down cells were suppressed to 20% or less at 24 – 96 h after transfection with siRNA as compared with that of control cells (Fig.5A). The apoptotic fraction of HepG2 cells transfected with PUMA siRNA was 22.7 ± 3.5%, which was significantly lower than that of control cells (46.5 ± 3.6%) (p<0.01 by Student's t test; Fig.5B). Similarly, the apoptotic fraction of HuH-7 cells transfected with PUMA siRNA (37.0 ± 2.6%) was significantly lower than that of control siRNA (45.9 ± 2.6%) (p<0.01; Fig.5C). Thus, knockdown of PUMA resulted in escape from apoptosis by the combination of DPC and X-ray irradiation in both HepG2 and HuH-7 cells. In addition, knockdown of PUMA decreased most strongly the cytotoxic activity of DPC plus X-ray irradiation among the treatments (vehicle, DPC, X-ray alone and DPC/X-ray combination), in both cell lines, suggesting that PUMA may play an important role in the synergistic effect of this combination as well as in apoptosis induction (Supplementary Table 2).

Cell cycle arrest with DPC or CDDP plus X-ray irradiation

To investigate the effects of DPC or CDDP plus X-ray irradiation on the cell cycle, we quantified cell subpopulations in sub-G1, G0/1, S, and G2/M phases after treatment with DPC/CDDP and/or X-ray by flow cytometry. DPC treatment significantly increased the sub-G1 population in HepG2 cells (65.6 ± 1.5%) compared with control

cells (26.8 ± 1.7%; p<0.01 by Dunnett's test; Fig.6A), indicative of apoptosis induction. In contrast, X-ray irradiation significantly increased the G2/M phase population in HepG2 cells (30.7 ± 1.1%) compared with control cells (25.7 ± 0.7%; p<0.01), suggesting G2/M arrest. DPC plus X-ray irradiation significantly increased the apoptotic sub-G1 population (70.2 ± 0.6%; p<0.01). Similar patterns were observed in HepG2 cells treated with CDDP, and with CDDP plus X-ray irradiation. In contrast, experiments with HuH-7 cells showed that DPC significantly increased the S phase population (44.5 ± 5.7% vs 11.1 ± 0.6% for control; p<0.01; Fig.6B) as well as sub-G1 population (6.7 ± 0.4% vs 4.3 ± 0.6% for control; p<0.01), and X-ray irradiation induced sub-G1 (8.1 ± 0.9%; p<0.01) and G2/M arrest (37.3 ± 0.5% vs 25.3 ± 0.8% for control; p<0.01). DPC plus X-ray irradiation significantly induced the S phase (29.1 ± 3.7%; p<0.01), sub-G1 (8.2 ± 0.6%; p<0.01), and G2/M phase populations (34.3 ± 1.0%; p<0.01) in HuH-7 cells. While CDDP increased the sub-G1 (9.7 ± 0.4%; p<0.01) and G0/G1 population (72.2 ± 3.0% vs 59.4 ± 0.4% for control; p<0.01), possibly leading to apoptosis. CDDP plus X-ray irradiation increased only the apoptotic sub-G1 population (7.8 ± 0.8%; p<0.01). Thus, the effect of DPC on the cell cycle in HuH-7 cells differed from that of CDDP.

Subsequently a BrdU incorporation assay was performed to determine DNA synthetic activity in HepG2 and HuH-7 cells treated with DPC, X-ray irradiation, and both in combination. Representative data are shown in Fig.6C. Both DPC and X-ray irradiation significantly decreased the number of BrdU-incorporated cells in both cell lines. The combination of DPC plus X-ray irradiation decreased DNA synthetic activity most strongly (up to 0.5 - 1.0%) in both cell lines. It is expected that not only HepG2 cells but also HuH-7 cells, which showed S phase arrest, would undergo subsequent apoptosis as described previously [26].

To examine the expression of cell cycle regulators, we performed western blotting for cyclins A, B1, D1, and E (Fig.6D). DPC or DPC plus X-ray irradiation decreased cyclin D1 expression strongly in HepG2 cells, which may be associated with an increased sub-G1 population [27]. X-ray irradiation caused cyclin B1 accumulation in both cell types, consistent with G2/M arrest in those cells [28]. Moreover, DPC or DPC plus X-ray irradiation decreased cyclins A and E in p53 wild-type HepG2 cells, also consistent with previous reports [29, 30]. However, considerably weaker effects of CDDP plus X-ray irradiation on those cyclins were observed compared with DPC plus X-ray irradiation.

Effect of miriplatin plus X-ray irradiation on locally advanced HCC

To evaluate the therapeutic efficacy of miriplatin plus radiotherapy on locally advanced HCC, we retrospectively compared the therapeutic efficacy of miriplatin-TACE plus radiotherapy versus CDDP-TACE plus radiotherapy for locally advanced HCC patients with macroscopic vascular and/or bile duct invasion. The baseline characteristics of the patients are summarized in Supplementary Table 3, and more detailed information is provided in Supplementary Table 4. No significant differences in characteristics including age; sex; etiology; laboratory data; liver functional reserve; and tumor size, number, degree of vascular/bile duct invasion, and stage were observed between the miriplatin and CDDP groups. Representative CT images of CR, PR, SD and PD for primary evaluation of the main tumor with vascular/bile duct invasion inside the radiation field are shown in Fig.7A-D. The HCC tumor invading the portal vein completely disappeared in case 9 (CR), and the tumor invading the portal vein shrank but still remained in case 4 (PR) after treatment with miriplatin-TACE and radiotherapy. However, the tumor invading the portal vein showed little change in case

21 (SD), and the tumor invading the portal vein progressed in case 24 (PD) after treatment with CDDP-TACE and radiotherapy. In total, the overall RR in the miriplatin group (100% [10/10]; 8 CR and 2 PR) was significantly higher than in the CDDP group (53.3% [8/15]); 6 CR, 2 PR, 5 SD, 2 PD; $p<0.05$; Fig.7E), despite the small number of patients. We also evaluated secondarily intrahepatic nodules outside the radiation field based on modified RECIST criteria; the RR in the miriplatin group was 30% (3/10; 2 CR, 1 PR, 2 SD, 5 PD), and was similar to that in the CDDP group (40% [6/15]; 5 CR, 1 PR, 6 SD, 3 PD; Supplementary Table 5). OS in the miriplatin group (23.6 months; 95% CI 6.9 – 33.3) was fairly higher than in the CDDP group (10.4 months; 95% CI 4.4 – 21.6), although the difference was not statistically significant ($p=0.16$ by log rank test; Fig.7F). These results may suggest that the tumor with vascular/bile duct invasion determined the prognosis (OS) in locally advanced HCC, as described previously [7]. Thus, our data suggest that combination treatment with miriplatin and X-ray irradiation may possibly be more effective against locally advanced HCC compared with CDDP-TACE plus radiotherapy.

Discussion

In this study, we demonstrated that miriplatin and X-ray irradiation in combination has a synergistic effect on HCC cells. This is the first study to have investigated the anti-tumor activity of miriplatin plus X-ray irradiation in vitro and in vivo. We also showed that this combination caused strong apoptosis mediated via PUMA expression. Synergistic induction of PUMA in HCC cells after treatment with the combination, and inhibition of apoptosis by knocking down the PUMA gene in HCC cells, indicate a pivotal role of PUMA in apoptosis caused by the combined treatment. Moreover, TACE with miriplatin concurrently combined with radiotherapy showed a high response rate

in patients with unresectable HCC invading macroscopically portal/hepatic veins and/or bile ducts, despite a limited number of patients studied. Conversely, CDDP showed little synergistic effect on HCC cell lines nor did it induce PUMA to trigger apoptosis.

PUMA is a key molecule for apoptosis induction by anti-tumor drugs and by radiotherapy. The expression of PUMA is reportedly elevated in response to DNA-damaging stimuli through p53-dependent or p53-independent transcription. It has been reported that X-ray irradiation enhances PUMA expression mainly through p53-dependent transcription activation, leading to apoptosis in oral cancer, nasopharyngeal cancer, and breast cancer [31]. However, no published studies have investigated the mechanism of apoptosis induced by miriplatin. Notably, oxaliplatin, whose active form, DPC, is the same as miriplatin, enhances PUMA expression in colorectal cancer [32]. Although it is unclear how radiation and DPC exert synergistic anti-tumor activity in detail, it is plausible that the combination of miriplatin and X-ray irradiation synergistically enhances PUMA expression, leading to strong induction of apoptosis in HCC cells. In addition, we used the 2 cell lines, HepG2 with p53 wild and HuH-7 with p53 mutant, and both lines showed similarly enhanced PUMA expression after treatment with DPC plus X-ray irradiation, possibly leading to induction of apoptosis.

Eventually, DPC increased PUMA and cleaved PARP expression levels similarly in a dose-dependent manner in HepG2 and HuH-7 cells. Notably, their expression levels started to increase at lower DPC concentrations (0 – 1.25 μM) in HuH-7 cells than in HepG2 cells (2.5 – 5.0 μM; Supplementary Fig.2). These results are consistent

with the difference in IC50 of these cells for DPC, and also suggest a close association of PUMA with apoptosis in both cells.

Regarding the mechanism of PUMA induction, we found enhanced p-JNK and p-c-JUN expression but not ER stress-related protein (CHOP) expression in both cell lines after treatment with DPC plus X-ray irradiation (Fig.4E,F). These results suggest that DPC plus X-ray irradiation induced PUMA expression via the JNK signaling pathway, consistent with a previous report on JNK-dependent PUMA induction [33]. It is also assumed that induced PUMA activates Bax and Bak, leading to activation of the caspase cascade and ultimately to cell apoptosis. Thus, the combination of miriplatin and X-ray irradiation would be effective on HCC cells regardless of the status of p53 mutation. In addition, the PUMA mRNA expression level was significantly lower in primary normal hepatocytes compared with HCC cells, and the difference in expression was enhanced roughly tenfold after treatment with DPC and X-ray irradiation (Supplementary Fig.4). These data suggest that DPC plus X-ray irradiation would be selectively effective against HCC cells without affecting mostly normal hepatocytes.

Cisplatin, a hydrophilic agent like most other chemotherapeutic agents, is commonly used for TACE with or without radiation therapy in patients with HCC [34]. A retrospective analysis by Oguro and associates reported that TACE with miriplatin demonstrated a significantly lower response rate but lower rates of adverse events than TACE with CDDP [35]. In their report, however, the mean dose of miriplatin administered (50.4 mg, 64.4 μmol) was lower than that of CDDP (55.9 mg, 186.3 μmol). In our study, the IC50 value of DPC (miriplatin) in HCC cell lines was significantly lower than that of CDDP. Therefore, it is plausible that miriplatin has stronger anti-tumor

activity than CDDP against HCC at quimolar doses. It remains controversial as to whether or not the combination of CDDP and radiation has a synergistic effect [36,37]. However, our results indicated that CDDP plus X-ray showed little synergy. This may be related to the fact that CDDP did not induce PUMA expression in cancer cells as revealed by our group (Supplementary Fig.2) and other investigators [39].

In addition to analysis of apoptosis to determine the mechanism underlying the effect of miriplatin in combination with radiation, we also analyzed the effects of DPC (miriplatin) plus radiation on cell cycle arrest by flow cytometry (Fig.6). DPC alone induced sub-G1 arrest in HepG2 cells with wild-type p53, probably leading to p53 dependent apoptosis. In contrast, DPC alone mainly induced S phase arrest as well as sub-G1 arrest in HuH-7 cells with mutant p53, which is consistent with previous studies showing that several anti-cancer drugs induce S phase arrest in cancer cells, subsequently leading to apoptosis [26]. Interestingly, our results are also compatible with a previous report showing that zolendronic acid induced PUMA and S phase arrest in cancer cells [39]. On the other hand, X-ray irradiation alone induced G2/M arrest in these cell lines, consistent with previous reports [28]. The combination of DPC plus irradiation induced both sub-G1 and S phase arrest and a much greater degree of G2/M arrest in HCC cells. In our study, DPC alone decreased cyclin D1 expression, while X-ray irradiation caused cyclin B1 accumulation, consistent with previous reports [28, 40]. Thus, cell cycle arrest might be associated with the synergistic effect of DPC and X-ray irradiation.

In preliminary experiments, we investigated invasion capability in 5 HCC cell lines (HepG2, HuH-7, PLC/PRF5, HuH-1, and Hep3B) using a transwell invasive assay. HepG2 and HuH-7 cells showed the highest invasion activities, followed by HuH-1,

PLC/PRF5, and Hep3B cells (Supplementary Fig.5A,B). Moreover, HepG2 and HuH-7 cells were p53 wild and mutant, respectively, and thus it appears that HepG2 and HuH-7 cells were suitable for the current experiments. In addition, when HepG2 and HuH-7 cells were treated with DPC plus X-ray irradiation, invasion activity was significantly decreased compared with control cells after correction for viable cell numbers (p<0.05; Supplementary Fig.5C-E).

Our retrospective analyses of miriplatin plus radiotherapy showed a higher response rates of the main tumor with vascular/bile duct invasion and longer OS times in locally advanced HCC than those of CDDP plus radiotherapy, despite the small number of patients. These values were also greater than those previously reported for CDDP plus radiotherapy [13, 14]. The total radiation doses in previous reports of CDDP plus radiotherapy ranged from 37.5 – 45 Gy, which is lower than the dose used in our study (50 Gy). The dose of CDDP in previous reports was 2 mg/kg (6.7 μmol/kg) whereas the dose of miriplatin in our study was 2 mg/kg (2.6 μmol/kg). Consequently, it appears that the synergistic effect of miriplatin and radiotherapy in this study might be attributable to the high RR of the main tumor. In addition, no grade 3/4 adverse event was observed in the miriplatin group, although grade 3/4 adverse events were observed at a rate of 53.3% (8/15) in the CDDP group (Supplementary Table 6), consistent with previous reports showing that miriplatin is much less toxic than cisplatin [41].

A limitation of this study is that the human data on miriplatin-TACE and CDDP-TACE with radiotherapy are small sample-sized and retrospective analysis. Therefore, a prospective large-scale study to compare those therapies should be performed in the future.

In conclusion, our data suggest that combination treatment with miriplatin and X-ray irradiation has a synergistic effect on HCC cells, and that this combination induces PUMA-mediated apoptosis as well as cell cycle arrest in HCC cells, regardless of the status of p53 mutation. Our results suggest that TACE with miriplatin combined with radiotherapy may be possibly effective for locally advanced HCC.

Acknowledgements

We are grateful to Misato Hirata and Masahiro Bando for their technical assistance.

Competing interests: Tetsuji Takayama received DPC from Sumitomo Dainippon Pharma Co, Ltd. (Osaka Japan) in this study.

Funding: This work was partly supported by a Grant-in-Aid for Scientific Research from the Japan Society for the Promotion of Science (JSPS; grant number 17K15950).

References

1. Bray F, Ferlay J, Soerjomataram I, et al. Global cancer statistics 2018: GLOBOCAN estimates of incidence and mortality worldwide for 36 cancers in 185 countries. CA Cancer J Clin. 2018;68:394-424.
2. Llovet JM, Real MI, Montaña X, et al. Arterial embolisation or chemoembolisation versus symptomatic treatment in patients with unresectable hepatocellular carcinoma: a randomised controlled trial. Lancet. 2002;359:1734-9.
3. Llovet JM, Bruix J. Systematic review of randomized trials for unresectable hepatocellular carcinoma: Chemoembolization improves survival. Hepatology. 2003;37:429-42.
4. Llovet JM, Ricci S, Mazzaferro V, et al. Sorafenib in advanced hepatocellular carcinoma. N Engl J Med. 2008;359:378-90.
5. Kudo M, Finn RS, Qin S, et al. Lenvatinib versus sorafenib in first-line treatment of patients with unresectable hepatocellular carcinoma: a randomised phase 3 non-inferiority trial. Lancet. 2018;391:1163-73.
6. Bruix J, Qin S, Merle P, et al. Regorafenib for patients with hepatocellular carcinoma who progressed on sorafenib treatment (RESORCE): a randomised, double-blind, placebo-controlled, phase 3 trial. Lancet. 2017;389:56-66.
7. Cabibbo G, Enea M, Attanasio M, et al. A meta-analysis of survival rates of untreated patients in randomized clinical trials of hepatocellular carcinoma. Hepatology. 2010;51:1274-83.
8. Masuda K, Ono A, Aikata H, et al. Serum HMGB1 concentrations at 4 weeks is a useful predictor of extreme poor prognosis for advanced hepatocellular carcinoma treated with sorafenib and hepatic arterial infusion chemotherapy. J Gastroenterol. 2018;53:107-18.
9. Cheng AL, Guan Z, Chen Z, et al. Efficacy and safety of sorafenib in patients with advanced hepatocellular carcinoma according to baseline status: subset analyses of the phase III Sorafenib Asia-Pacific trial. Eur J Cancer. 2012;48:1452-65.
10. Zeng ZC, Fan J, Tang ZY, et al. A comparison of treatment combinations with and without radiotherapy for hepatocellular carcinoma with portal vein and/or inferior vena cava tumor thrombus. Int J Radiat Oncol Biol Phys. 2005;61:432-43.
11. Huang YJ, Hsu HC, Wang CY, et al. The treatment responses in cases of radiation therapy to portal vein thrombosis in advanced hepatocellular carcinoma. Int J Radiat Oncol Biol Phys. 2009;73:1155-63.
12. Yamada K, Izaki K, Sugimoto K, et al. Prospective trial of combined transcatheter arterial chemoembolization and three-dimensional conformal radiotherapy for portal vein tumor thrombus in patients with unresectable hepatocellular carcinoma. Int J Radiat Oncol Biol Phys. 2003;57:113-9.
13. Yoon SM, Lim YS, Won HJ, et al. Radiotherapy plus transarterial chemoembolization for hepatocellular carcinoma invading the portal vein: long-term patient outcomes. Int J Radiat Oncol Biol Phys. 2012;82:2004-11.
14. Yoon SM, Ryoo BY, Lee SJ, et al. Efficacy and Safety of Transarterial Chemoembolization Plus External Beam Radiotherapy vs Sorafenib in Hepatocellular Carcinoma With Macroscopic Vascular Invasion: A Randomized Clinical Trial. JAMA Oncol. 2018;4:661-9.
15. Pabla N, Dong Z. Cisplatin nephrotoxicity: mechanisms and renoprotective strategies. Kidney Int. 2008;73:994-1007.
16. Hanada M, Baba A, Tsutsumishita Y, et al. Intra-hepatic arterial administration with miriplatin suspended in an oily lymphographic agent inhibits the growth of tumors implanted in rat livers by inducing platinum-DNA adducts to form and massive apoptosis. Cancer Chemother Pharmacol. 2009;64:473-83.
17. Okusaka T, Okada S, Nakanishi T, et al. Phase II trial of intra-arterial chemotherapy using a novel lipophilic platinum derivative (SM-11355) in patients with hepatocellular carcinoma. Invest New Drugs. 2004;22:169-76.

18. Imai Y, Chikayama T, Nakazawa M, et al. Usefulness of miriplatin as an anticancer agent for transcatheter arterial chemoembolization in patients with unresectable hepatocellular carcinoma. J Gastroenterol. 2012;47:179-86.
19. Ikeda M, Kudo M, Aikata H, et al. Transarterial chemoembolization with miriplatin vs. epirubicin for unresectable hepatocellular carcinoma: a phase III randomized trial. J Gastroenterol. 2018;53:281-90.
20. Chou TC. Drug combination studies and their synergy quantification using the Chou-Talalay method. Cancer Res. 2010;70:440-6.
21. Liao B, Zhang Y, Sun Q, et al. Vorinostat enhances the anticancer effect of oxaliplatin on hepatocellular carcinoma cells. Cancer Med. 2018;7:196-207.
22. Okada Y, Kimura T, Nakagawa T, et al. EGFR Downregulation after Anti-EGFR Therapy Predicts the Antitumor Effect in Colorectal Cancer. Mol Cancer Res. 2017;15:1445-54.
23. Onishi H, Nouso K, Nakamura S, et al. Efficacy of hepatic arterial infusion chemotherapy in combination with irradiation for advanced hepatocellular carcinoma with portal vein invasion. Hepatol Int. 2015;9:105-12.
24. Eisenhauer EA, Therasse P, Bogaerts J, et al. New response evaluation criteria in solid tumours: revised RECIST guideline (version 1.1). Eur J Cancer. 2009;45:228-47.
25. Shen D, Wang H, Zheng Q, et al. Synergistic effect of a retinoid X receptor-selective ligand bexarotene and docetaxel in prostate cancer. Onco Targets Ther. 2019;12:7877-86.
26. Shapiro GI, Harper JW. Anticancer drug targets: cell cycle and checkpoint control. J Clin Invest. 1999;104:1645-53.
27. Kranenburg O, van der Eb AJ, Zantema A. Cyclin D1 is an essential mediator of apoptotic neuronal cell death. EMBO J. 1996;15:46-54.
28. Lin ZZ, Chou CH, Cheng AL, et al. Radiosensitization by combining an aurora kinase inhibitor with radiotherapy in hepatocellular carcinoma through cell cycle interruption. Int J Cancer. 2014;135:492-501.
29. Voland C, Bord A, Péleraux A, et al. Repression of cell cycle-related proteins by oxaliplatin but not cisplatin in human colon cancer cells. Mol Cancer Ther. 2006;5:2149-57.
30. Jiang T, Zhang H, Liu X, et al. Effect of oxaliplatin combined with polyenephosphatidylcholine on the proliferation of human gastric cancer SGC-7901 cells. Oncol Lett. 2016;12:4538-46.
31. Yu J, Zhang L. PUMA, a potent killer with or without p53. Oncogene. 2008;27 Suppl 1:S71-83.
32. Wang X, Li M, Wang J, et al. The BH3-only protein, PUMA, is involved in oxaliplatin-induced apoptosis in colon cancer cells. Biochem Pharmacol. 2006;71:1540-50.
33. Cazanave SC, Mott JL, Elmi NA, et al. JNK1-dependent PUMA expression contributes to hepatocyte lipoapoptosis. J Biol Chem. 2009;284:26591-602.
34. Chung SR, Kim JH, Yoon HK, et al. Combined Cisplatin-Based Chemoembolization and Radiation Therapy for Hepatocellular Carcinoma Invading the Main Portal Vein. J Vasc Interv Radiol. 2015;26:1130-8.
35. Oguro S, Hashimoto S, Tanaka T, et al. Short-term therapeutic effects of transcatheter arterial chemoembolization using miriplatin-lipiodol suspension for hepatocellular carcinoma. Jpn J Radiol. 2012;30:735-42.
36. Chenoufi N, Raoul JL, Lescoat G, et al. In vitro demonstration of synergy between radionuclide and chemotherapy. J Nucl Med. 1998;39:900-3.
37. Kitabayashi H, Shimada H, Yamada S, et al. Synergistic growth suppression induced in esophageal squamous cell carcinoma cells by combined treatment with docetaxel and heavy carbon-ion beam irradiation. Oncol Rep. 2006;15:913-8.
38. Wang J, Zhou JY, Wu GS. Bim protein degradation contributes to cisplatin resistance. J Biol Chem. 2011;286:22384-92.
39. Liu SS, Wang XP, Li XB, et al. Zoledronic acid exerts antitumor effects in NB4 acute promyelocytic leukemia cells by inducing apoptosis and S phase arrest. Biomed Pharmacother. 2014;68:1031-6.

40. Qu K, Xu X, Liu C, et al. Negative regulation of transcription factor FoxM1 by p53 enhances oxaliplatin-induced senescence in hepatocellular carcinoma. Cancer Lett. 2013;331:105-14.
41. Otsuji K, Takai K, Nishigaki Y, et al. Efficacy and safety of cisplatin versus miriplatin in transcatheter arterial chemoembolization and transarterial infusion chemotherapy for hepatocellular carcinoma: A randomized controlled trial. Hepatol Res. 2015;45:514-22.

Figure legends

Figure 1.

Viability of HCC cells treated with DPC and CDDP. A. HepG2 and HuH-7 cells were treated with DPC or CDDP for 72 h. Cell viability was then determined by WST-8 assay. IC50 values were calculated by non-linear regression analysis. Combination index analysis of DPC or CDDP combined with X-ray irradiation in HCC cells. HepG2 or HuH-7 cells were incubated with various concentrations of DPC (B, C) or CDDP (D, E) combined with X-ray exposure (0 – 10Gy) at a fixed ratio. After 120 h, cell viability was determined by WST-8 assay. The CI was calculated as described in Materials and Methods. A CI value <1 and >1 indicates synergistic and antagonistic effects, respectively.

Figure 2.

Colony formation in HCC cells after exposure to DPC and X-ray irradiation. A, C. Representative images of colony formation in HepG2 (A) and HuH-7 cells (C). Cells were treated with DPC (250 nmol/L) with or without X-ray irradiation (1 Gy), followed by incubation for 14 days. They were then fixed with methanol and stained with 0.4% crystal violet. B, D. The number of colonies in HepG2 (B) and HuH-7 cells (D) with greater than 50 cells was determined and expressed as a percentage of the number of control cells. Data represent mean ± standard deviation (SD) of triplicated experiments. * $p < 0.05$ by Turkey's test.

Figure 3.

Apoptosis induction in HCC cells after treatment with DPC (5 μM) or CDDP (10 μM) and/or X-ray irradiation (5 Gy). A. Cells were treated with vehicle, DPC, CDDP or X-

ray irradiation alone, or DPC/CDDP + X-ray, then solubilized and subjected to western blot analysis for cleaved PARP and caspase-3. β-actin was used as a loading control. B, C. Flow cytometric analysis of HepG2 (B) and HuH-7 cells (C) for annexin V-FITC and propidium iodide (PI) staining of cells treated with vehicle or DPC/CDDP + X-ray. Data represent mean ± SD of triplicate experiments. * $p < 0.01$ by Turkey's test.

Figure 4.

Expression of apoptosis-related protein, JNK signaling, and ER stress-related protein in HCC cells treated with DPC, CDDP, and X-ray irradiation. A, C. HepG2 (A) or HuH-7 cells (C) were treated with vehicle, DPC (5 μM), CDDP (5 μM), or X-ray (5 Gy) alone, or DPC/CDDP + X-ray, then solubilized and subjected to western blot analysis for BH3 only protein and Bcl-2 family protein. β-actin was used as a loading control. B, D. Each of the PUMA protein bands in HepG2 (B) and HuH-7 cells (D) was specifically quantified and normalized to β-actin using the Image J program (National Institutes of Health, Bethesda, MD). ** $p < 0.05$ vs other treatment groups by Turkey test. E, F. Western blot analysis was performed for JNK, p-JNK, c-Jun, p-c-Jun, and CHOP protein in HepG2 (E) and HuH-7 cells (F) after treatment with DPC/CDDP plus X-ray irradiation.

Figure 5.

Knockdown of the PUMA gene resulted in escape from apoptosis by DPC and X-ray irradiation in HCC cells. A. The PUMA gene in HepG2 and HuH-7 cells was knocked down by siRNA. The relative mRNA levels at 24, 48, 72 and 96 h were determined by Taqman PCR. * $p < 0.01$. B, C. HepG2 (B) or HuH-7 cells (C) were transfected with siRNA against PUMA or control siRNA and treated with DPC (5 μM) plus X-ray

irradiation (5 Gy). Flow cytometric analysis for annexin V-FITC as well as for propidium iodide (PI) was performed. The percentages of annexin V-positive cells are presented as mean ± SD of triplicate experiments. $^{**}p < 0.01$ by Student's *t* test.

Figure 6.

Cell cycle analysis in HCC cells after exposure to DPC or CDDP and X-ray irradiation. A, B. Cell cycle profile of HCC cells treated with DPC (5 μM) or CDDP (5 μM) and/or X-ray irradiation (5 Gy). HepG2 (A) and HuH-7 cells (B) were treated with vehicle, DPC, CDDP, X-ray irradiation alone, or DPC or CDDP plus X-ray irradiation, and cell cycle profile was analyzed after 24 h by flow cytometry. **; $p < 0.01$ by Dunnett's test. C. HepG2 and HuH-7 cells were treated with vehicle, DPC or X-ray irradiation alone, or DPC plus X-ray irradiation, and BrdU incorporation was analyzed after 24 h by flow cytometry. D. HepG2 and HuH-7 cells were treated with vehicle, DPC, CDDP, X-ray irradiation alone, DPC plus X-ray irradiation, or CDDP plus X-ray irradiation, and cyclin expression was analyzed after 24 h by western blotting.

Figure 7.

Response and survival of HCC with vascular/bile duct invasion to transarterial chemoembolization (TACE) with miriplatin or TACE with CDDP combined with radiotherapy. Representative CT images of CR, PR, SD, and PD before and after treatment. A. An abdominal CT scan during the portal-venous phase in case 9 with HCC invading the portal vein. The tumor and portal invasion completely disappeared (CR) after miriplatin-TACE with radiotherapy. B. An abdominal CT scan during the portal-venous phase in case 4 with tumor invading the portal vein. The tumor invading the portal vein shrank but still remained (PR) after miriplatin-TACE with radiotherapy.

C. The tumor invading portal vein showed little change (SD) in case 21 after CDDP-TACE with radiotherapy. D. The size of tumor invading portal vein enlarged (PD) in case 24 after CDDP-TACE with radiotherapy. E. Summary of response in miriplatin and CDDP groups. F. Overall survival of patients in the miriplatin and CDDP groups was estimated by Kaplan-Meier analysis and differences were evaluated by log rank test.

Supplementary Figure 1.

Anti-tumor effect of X-ray irradiation on HCC cells. A. HepG2 and HuH-7 cells were irradiated with X-rays at 0, 2.5, 5, 7.5 and 10 Gy. After 5 days, cell viability was analyzed by WST-8 assay. ED50 values were calculated by non-linear regression analysis. B. HCC cells were irradiated with X-rays at each dose, then solubilized after 5 days and subjected to western blot analysis for PARP.

Supplementary Figure 2.

Expression of apoptosis-related protein in HCC cells after treatment with DPC or CDDP. HepG2 (A) and HuH-7cells (B) were treated with DPC or CDDP at 0 - 20 μM for 48 h, then solubilized and subjected to western blot analysis for BH3 only protein and Bcl-2 family proteins. β-actin was used as a loading control.

Supplementary Figure 3.

Quantitation of apoptosis-related protein expression in HepG2 and HuH-7 cells. The expression levels of Bim, Blk, Noxa, Bcl-2, Mcl-1 and Bcl-xl protein in HepG2 (A) and

HuH-7 cells (B) detected by western blot analysis were specifically quantitated and normalized to β-actin using the Image J program.

Supplementary Figure 4.

The expression of PUMA mRNA in normal hepatocytes and HepG2 cells after treatment with DPC, X-ray irradiation, and DPC plus X-ray irradiation. Normal hepatocytes or HepG2 cells were treated with DPC plus X-ray irradiation, and PUMA mRNA expression levels were determined by Taqman PCR. N.S., not significant. *p < 0.01 by Turkey's test. **The relative mRNA level of PUMA in normal hepatocytes was significantly lower than in HepG2 cells. p < 0.01 by Student's t test.

Supplementary Figure 5.

Invasion capability of HCC cells treated with DPC and X-ray irradiation. A. The invasion capability of 5 HCC cell lines was determined by transwell assay. A representative image of each cell line is shown. B. Five randomly selected fields were imaged and the number of invading cells was counted as described in Supplementary information. **p < 0.01 by Turkey's test. C. HepG2 and HuH-7 cells were treated with vehicle alone or DPC plus X-ray irradiation, cultured for 48 h, and invasion assay was performed. Representative images of HepG2 and HuH-7 cells are shown. D,E. The mean numbers of invading cells in HepG2 and HuH-7 cells are shown. **p < 0.01 by Student's t test.

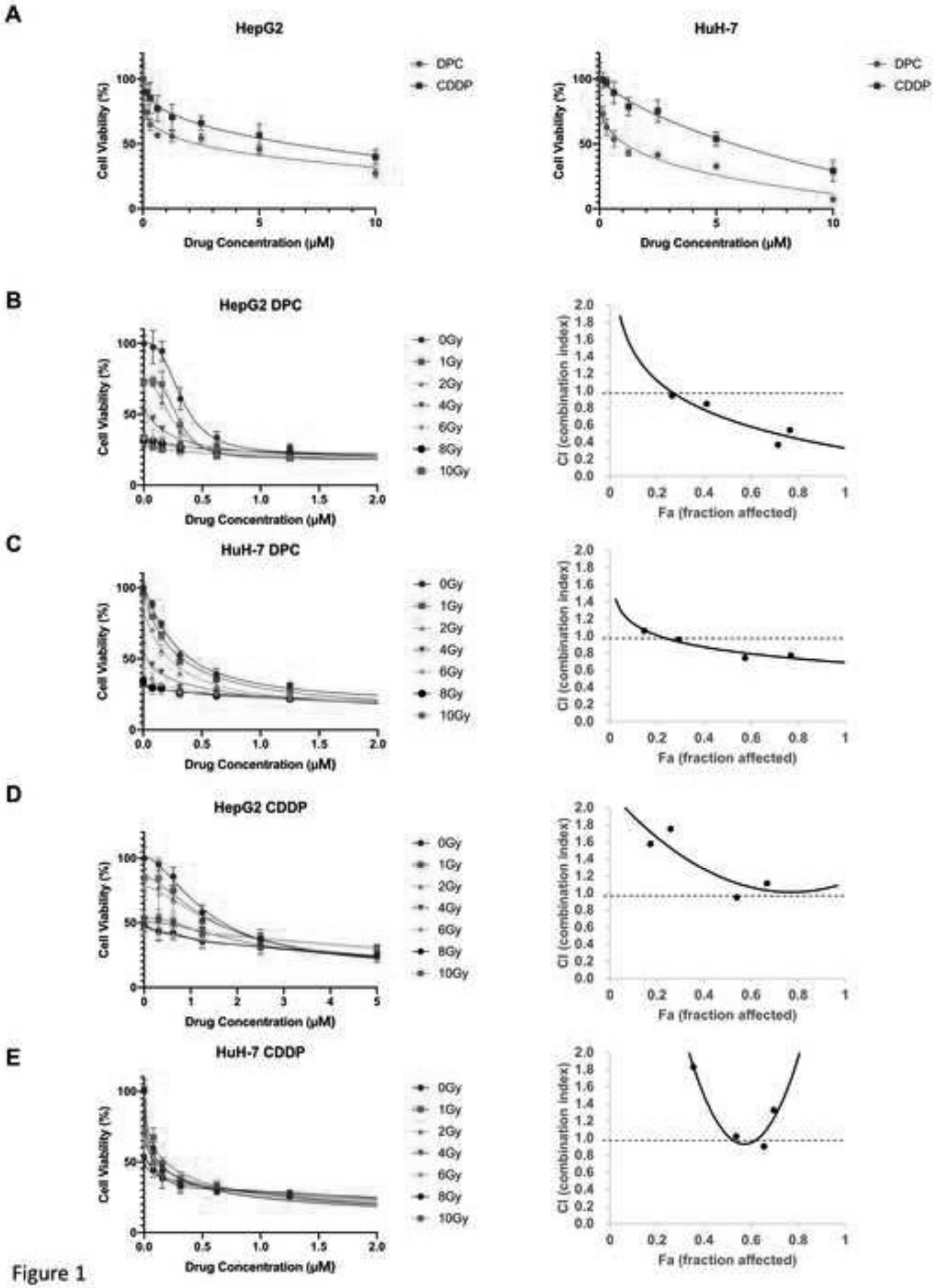

Figure 1

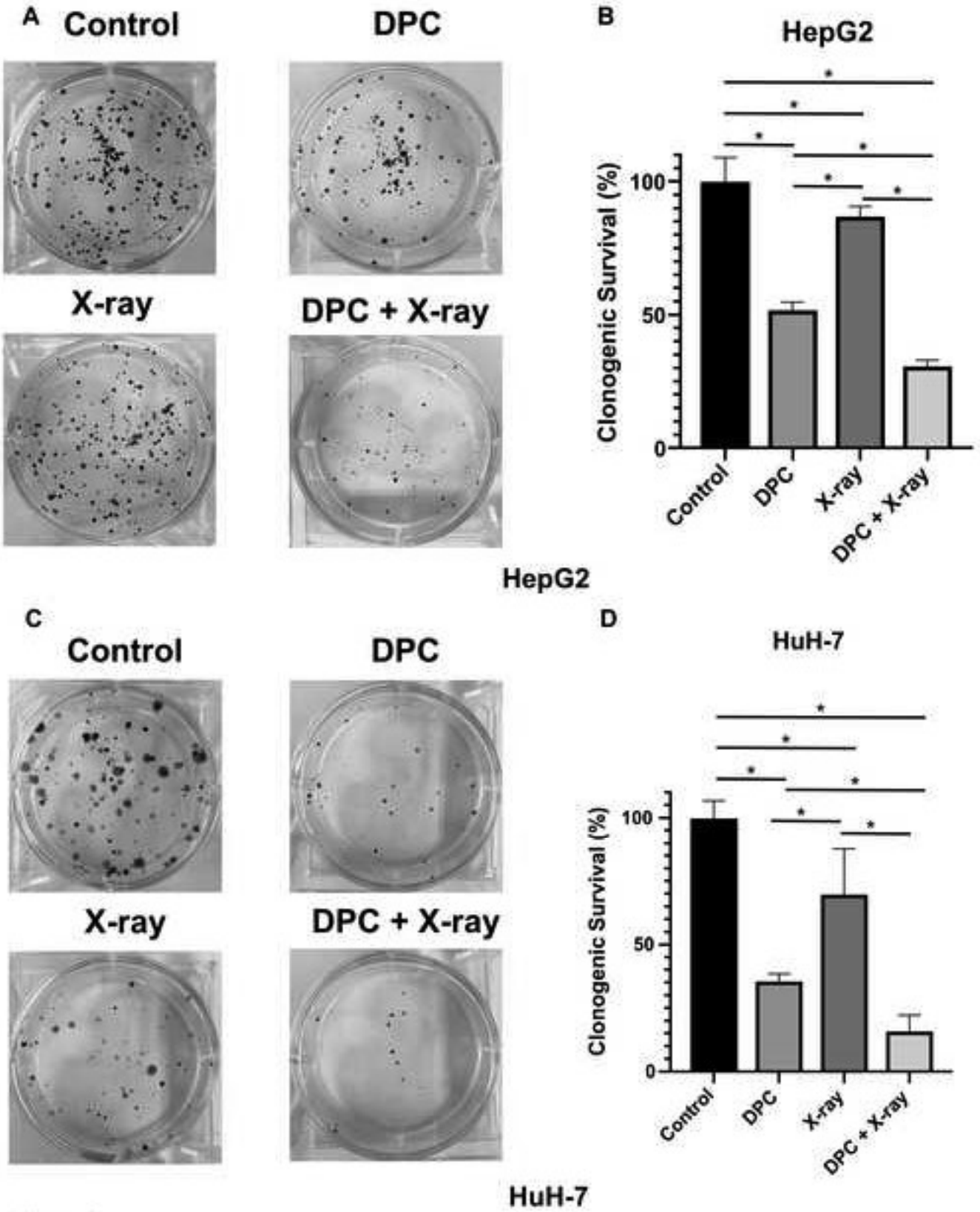

Figure 2

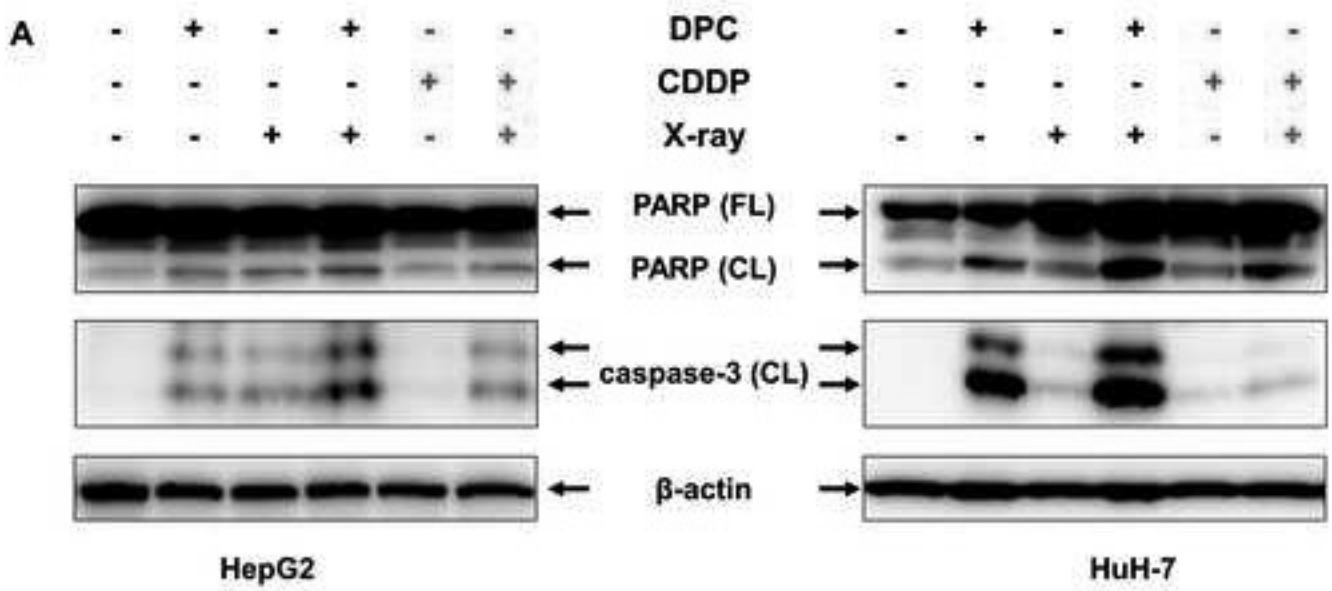
A
DPC
CDDP
X-ray
PARP (FL)
PARP (CL)
caspase-3 (CL)
β-actin
HepG2
HuH-7

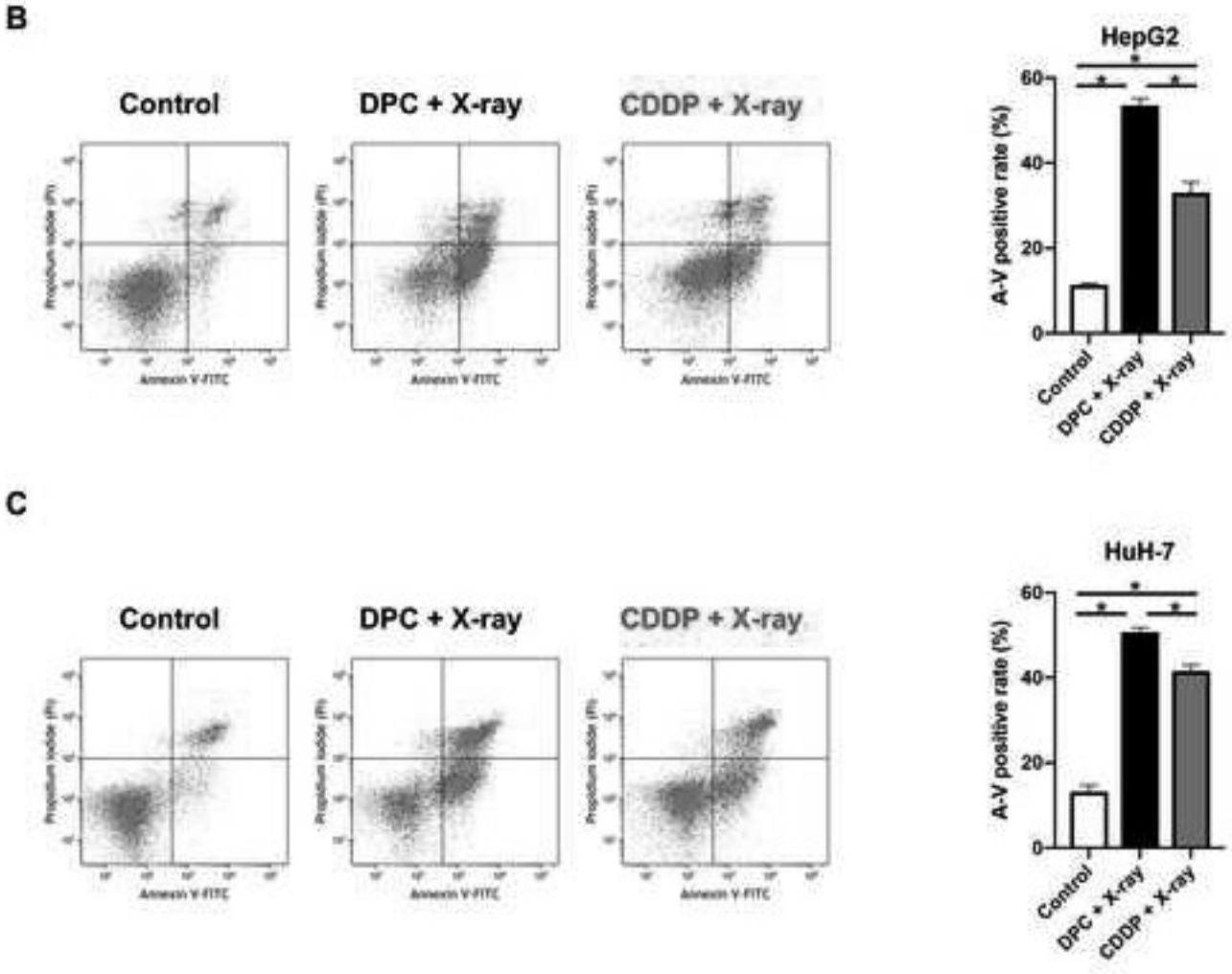
B
Control
DPC + X-ray
CDDP + X-ray
HepG2
A-V positive rate (%)
C
HuH-7

Figure 3

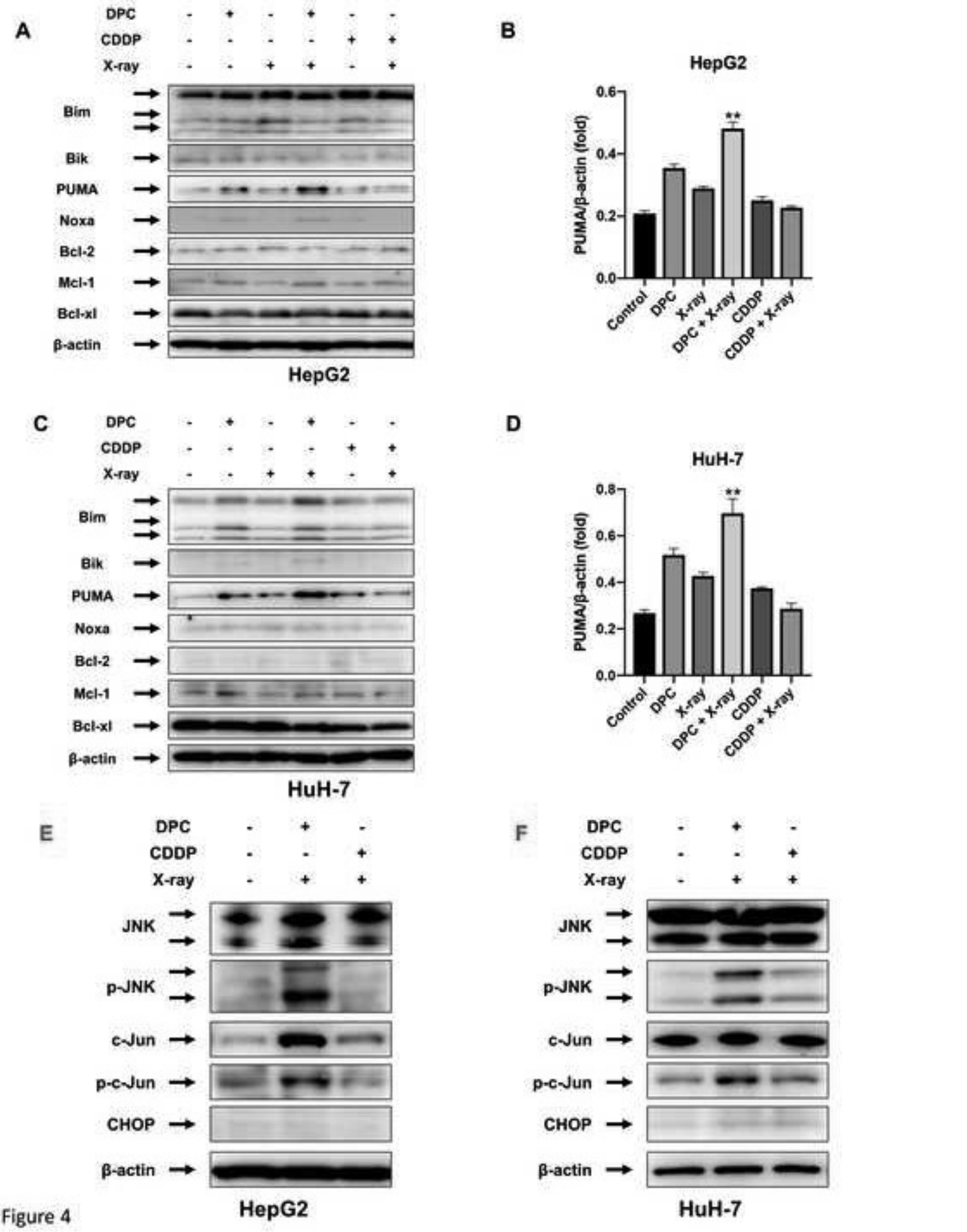

Figure 4

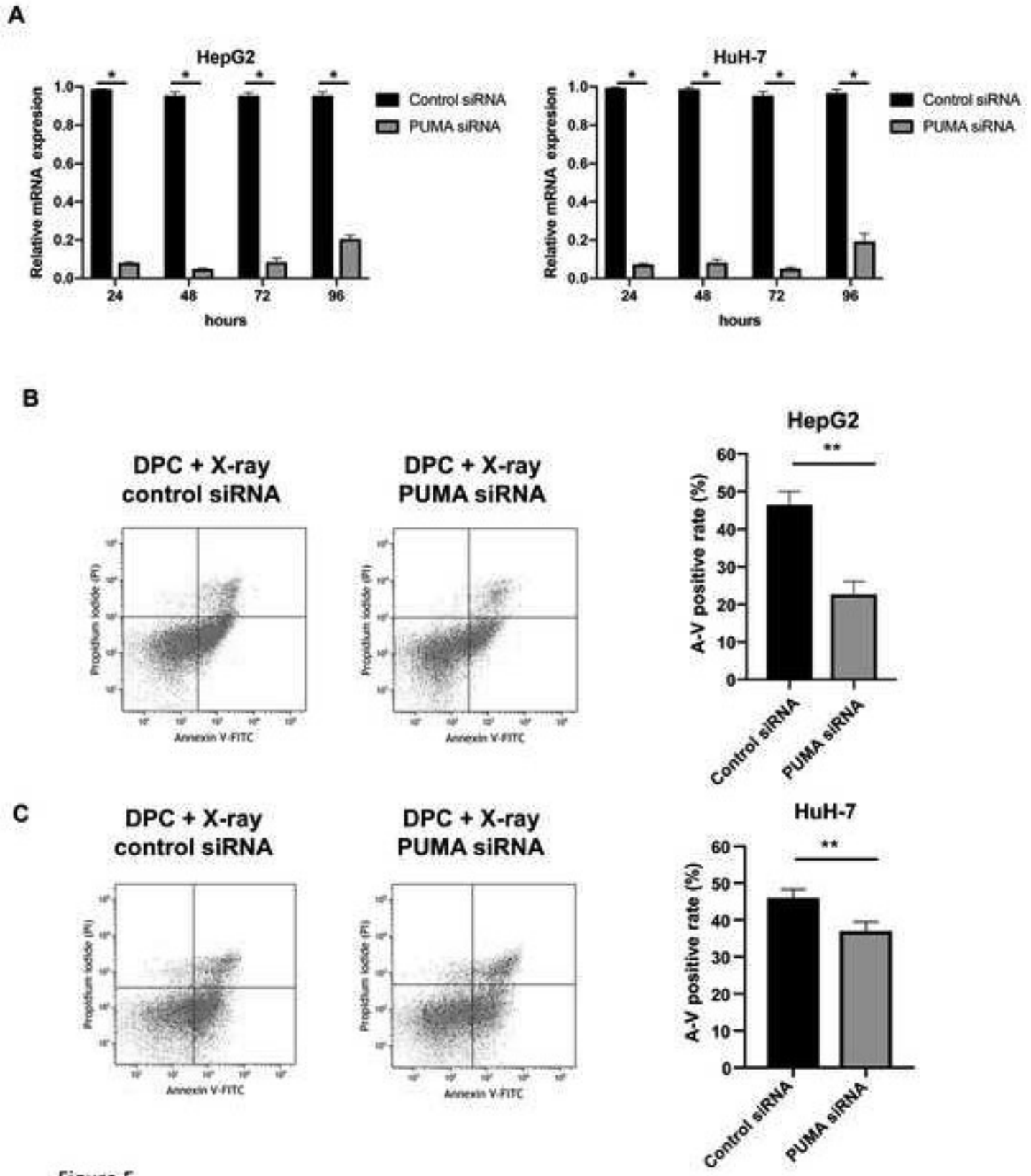
A
HepG2
HuH-7
Relative mRNA expression
1.0
0.8
0.6
0.4
0.2
0.0
24
48
72
96
hours
Control siRNA
PUMA siRNA
B
DPC + X-ray
control siRNA
DPC + X-ray
PUMA siRNA
Propidium Iodide (PI)
Annexin V-FITC
HepG2
A-V positive rate (%)
60
50
40
30
20
10
0
**
Control siRNA
PUMA siRNA
C
DPC + X-ray
control siRNA
DPC + X-ray
PUMA siRNA
Propidium Iodide (PI)
Annexin V-FITC
HuH-7
A-V positive rate (%)
60
50
40
30
20
10
0
**
Control siRNA
PUMA siRNA

Figure 5

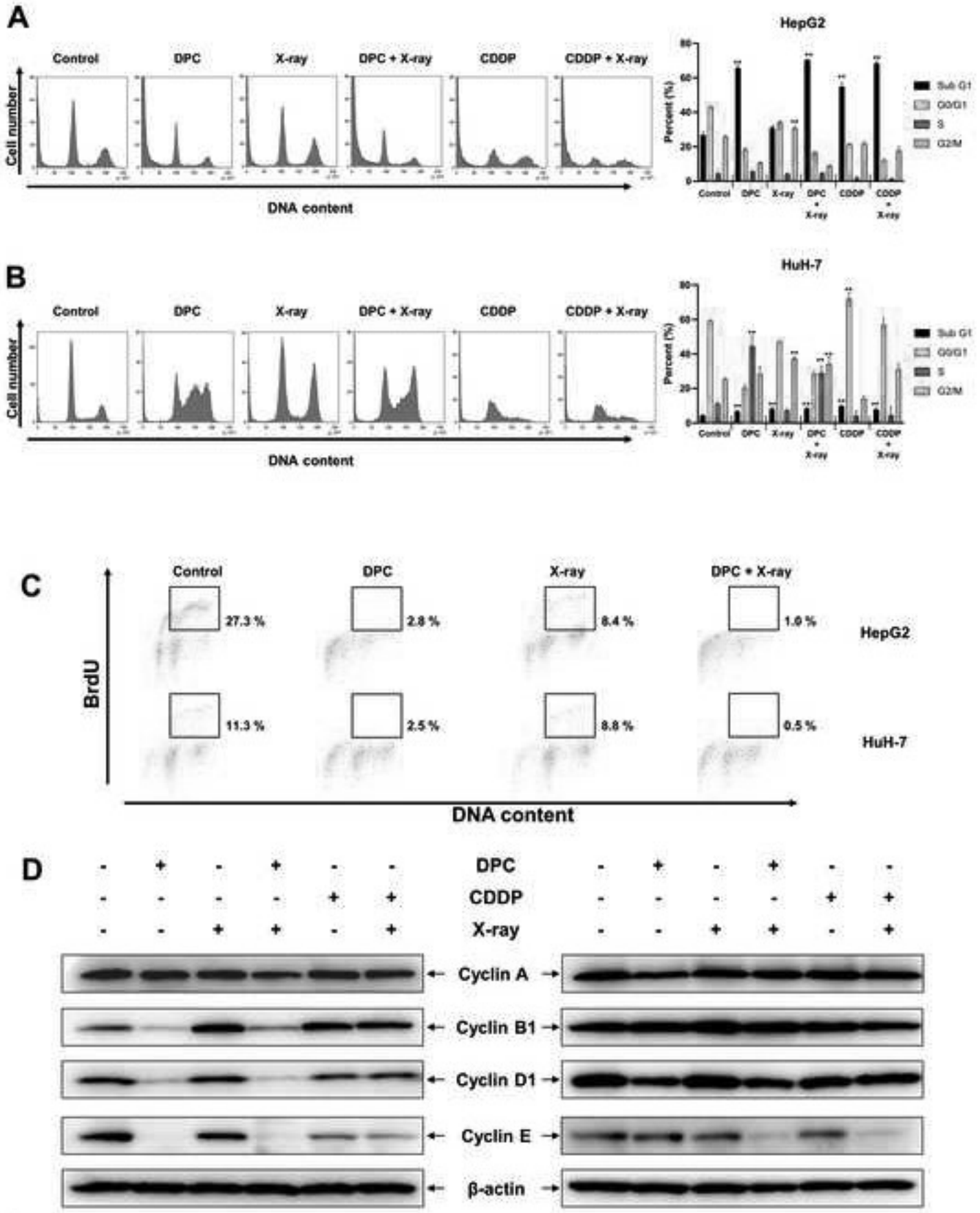

Figure 6

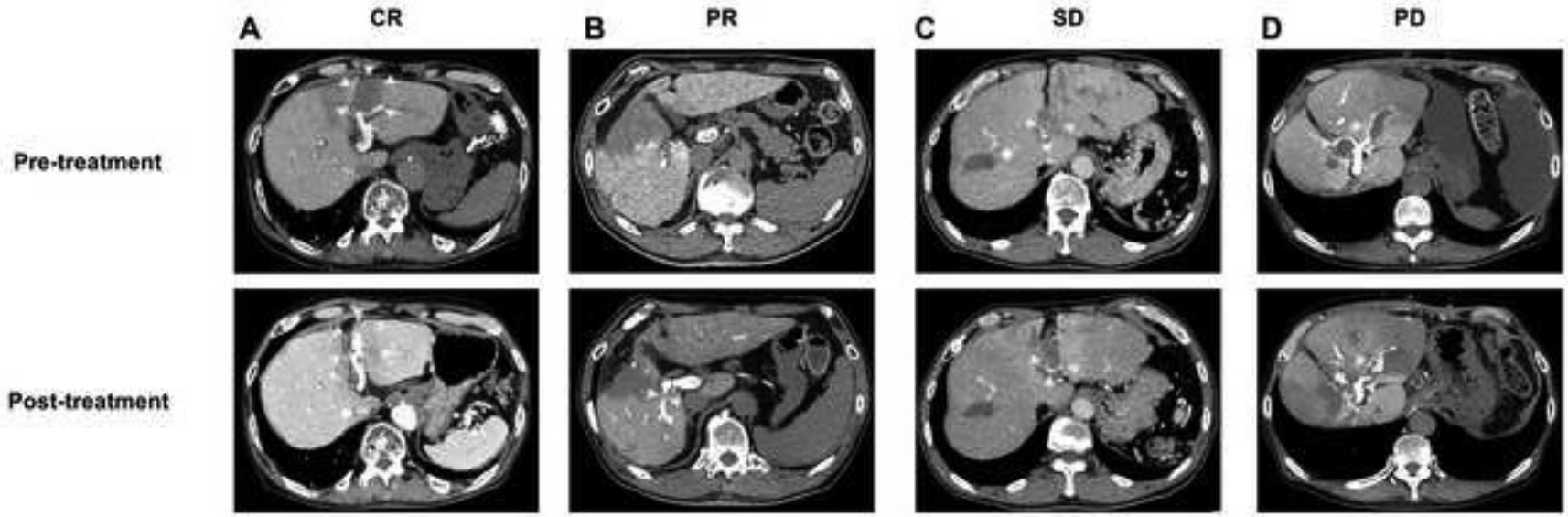

E

Response	Miriplatin group (n = 10)	Cisplatin group (n = 15)
Tumor invading portal vein/ hepatic vein/ bile duct		
CR	8 (80 %)	6 (40 %)
PR	2 (20 %)	2 (13 %)
SD	0 (0 %)	5 (33 %)
PD	0 (0 %)	2 (13 %)
RR (CR + PR) *	10 (100 %)	8 (53 %)

* p = 0.02

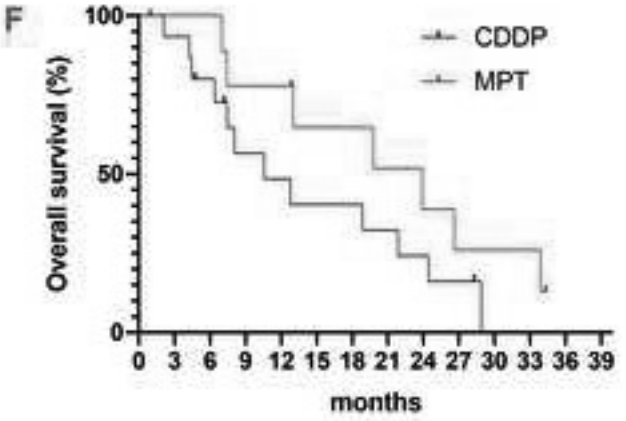

Figure 7